PCCP

Accepted Manuscript

ROYAL SOCIETY OF CHEMISTRY

www.rsc.org/pccp

Association of small aromatic molecules with PAMAM dendrimers

Ryan S. DeFever and Sapna Sarupria*

Department of Chemical & Biomolecular Engineering,

Clemson University, Clemson, SC 29634

Abstract

Many proposed applications using dendrimers, such as drug delivery and environmental remediation, involve dendrimer interactions with small molecules. Understanding the details of these interactions is important for designing dendrimers with tunable association with guest molecules. In this work, we investigate dendrimer interactions with small aromatic hydrocarbons using all-atom molecular dynamics simulations. We study the association of naphthalene (NPH) — the smallest polycyclic aromatic hydrocarbon — with 3^{rd}–6^{th} generation (G3–G6) polyamidoamine (PAMAM) dendrimers. Our work emphasizes that the association of small aromatic molecules with PAMAM dendrimers involves the formation of dynamic pocket-like association sites through interactions between flexible dendrimer branches and NPH molecules. The association sites are primarily formed by branches from the two outermost dendrimer subgenerations, and often involve the tertiary amine groups. Irrespective of their location on the dendrimer — whether buried or near the outer surface — these pocket-like structures lower the hydration of the associated NPH molecules. We show that on average NPH molecules with a lower hydration have a greater tendency to remain associated with the dendrimer for longer times. In general, the association sites are similar for the G3–G6 PAMAM dendrimers, indicating similarities in the association mechanisms across different dendrimer generations.

* ssarupr@g.clemson.edu

I. INTRODUCTION

Dendrimers are a class of branched synthetic macromolecules that offer defined, highly tunable structures with near monodispersity across a wide range of chemistries. Over 100 different dendrimer compositions have been synthesized,[1] and dendrimers have been studied in a plethora of research areas from pharmaceuticals to environmental remediation. Examples of proposed applications for dendrimers include drug delivery,[2–4] water purification,[5,6] and light harvesting.[7,8] In several of these applications dendrimer molecules interact with small aromatic hydrocarbons or molecules containing aromatic moieties. In drug delivery applications, dendrimers act as hosts for drug molecules, many of which contain aromatic rings.[9] For water purification, dendrimer-based nanosponges have been proposed to remove pollutants including polycyclic aromatic hydrocarbons.[5] Other applications undoubtedly involve dendrimer host–guest interactions with molecules involving aromatic entities. Previous studies have examined dendrimer host–guest interactions for a wide range of molecules, such as ibuprofen and phenobarbital.[10–13] Despite the abundance of studies examining dendrimer host–guest interactions, many studies are motivated by specific applications, and therefore focus on molecules which have a wide range of functionalities and several different types of intermolecular interactions with dendrimers. In our work we investigate the interactions between naphthalene (NPH) and generation 3 through generation 6 (G3–G6) polyamidoamine (PAMAM) dendrimers in order to gain insights into the interactions between small hydrophobic aromatic entities and dendrimers.

An extensive overview of studies that have investigated dendrimers and dendrimer host–guest interactions is beyond the scope of this introduction, so we limit our focus to relevant examples here and refer readers to other sources on the subject[10,14,15] for further information. Early work by Caminati et al. used a pyrene photoluminescence probe to sense the hydrophobicity of the local environment around associated pyrene molecules.[16] Despite the hydrophobicity of pyrene, the pyrene association sites were relatively hydrophilic for generation 0.5 to 9.5 PAMAM dendrimers. The authors observed a very small linear increase in the hydrophobicity of the association sites starting at generation 4.5, which they believed was related to increasing surface congestion for the larger dendrimers. High-generation triazine dendrimers hosting pyrene and camptothecin guest molecules showed a positive correlation between the guest capacity of the dendrimers

and the number of water molecules inside the dendrimers.[17] Together with the results of Caminati et al., it appears that a very hydrophobic dendrimer interior is not necessary for association of hydrophobic molecules. Jolly and Bonizzoni characterized the importance of various intermolecular interactions for encapsulation of small anionic molecules in G3–G6 PAMAM dendrimers.[18] Since these molecules were charged, they found electrostatic interactions (i.e., charge–charge, hydrogen bonding, and polar–π interactions) dominated the dendrimer–guest interactions. Many researchers have investigated the host–guest behavior of dendrimers with more complex molecules using NMR.[19–22] New techniques have allowed researchers to probe the locations of molecules within dendrimers, providing further insights into dendrimer host–guest interactions.[10] In one example, phenobarbital, a drug molecule with an aromatic moiety, associated with PAMAM dendrimers through both ionic interactions with the terminal groups and encapsulation.[12] Increasing dendrimer generation led to increased encapsulation of phenobarbital molecules and fewer ionic interactions with terminal groups. The authors proposed that increasing surface congestion both made backfolded terminal groups more difficult to access and provided increased hydrophobicity in the dendrimer interior, together making encapsulation more favorable. Along with many others, the studies outlined above show that dendrimers are able to encapsulate a variety of aromatic and hydrophobic molecules. However, it is challenging to probe the detailed mechanisms of association and encapsulation from experiments alone.

Molecular simulations offer the length scale resolution required to provide a molecular-level picture of dendrimer and guest behavior. Molecular dynamics (MD) simulations have been used to study dendrimers and their interactions with guest molecules.[23,24] Goddard and co-workers have extensively investigated the properties of G0–G10 PAMAM dendrimers in vacuum[25] and G4–G6 PAMAM dendrimers in the presence of explicit water solvent using MD simulations.[26–28] Tanis and Karatasos studied the association of ibuprofen with PAMAM dendrimers using MD simulations, reporting the mechanisms of formation for the dendrimer–drug complexes.[11] Their results emphasized the importance of hydrogen bonding and ionic interactions for ibuprofen–dendrimer complexes. Jain et al. compared the complexations of several drug molecules with dendrimers through potential of mean force and binding energy calculations.[29] From a comparison of the encapsulation ability of G4 PPI and G3 PAMAM dendrimers, the authors inferred that non-polar in-

teractions with dendrimer pockets was a primary mechanism of encapsulation. Previous simulation studies have focused on deciphering the types of intermolecular interactions governing host–guest behavior. It is expected that dendrimer structure and flexibility also play an important role in the host–guest interactions. What the local environment of the encapsulated guest molecules looks like and how the dendrimer encapsulates the guest molecules remain to be elucidated.

Motivated by these questions, we investigate the mechanisms of host–non-polar guest association through studies of the interactions of NPH with PAMAM dendrimers. Using NPH as our model guest molecule enables us to focus on the behavior of non-polar guests and non-polar moieties in dendrimer systems. We examine the molecular level details of the PAMAM dendrimer–guest interactions, including changes in the dendrimer structure, the location of NPH association within the dendrimer, and the local environment around NPH molecules which are associated with the dendrimer. The detailed description of NPH interactions with dendrimers developed through this work will provide a better understanding of how hydrophobic and aromatic moieties interact with PAMAM dendrimers in water, enabling better selection and tuning of dendrimer properties for specific applications.

II. METHODS

We performed MD simulations of G3–G6 PAMAM dendrimers and NPH in water to investigate the mechanisms of NPH association with dendrimer molecules. Each system consisted of one dendrimer, several NPH molecules, chlorine (Cl^-) counterions added to neutralize the system, and explicit water. The OPLS/AA force field[30] was used to describe the dendrimers, NPH molecules, and Cl^- counterions. Water was described by the TIP3P model.[31] Details of the OPLS/AA atom types used to describe the PAMAM dendrimers can be found in our previous work.[32]

A. Dendrimer Annealing Procedure

The initial dendrimer structures were obtained from Maiti et al.,[26] and the terminal amine groups were protonated to mimic PAMAM dendrimers at neutral pH conditions.[33]

Each dendrimer was solvated in water and the systems were neutralized with Cl^- counterions. The neutralized dendrimer–water systems were simulated for 21 ns in the isothermal-isobaric (NpT) ensemble at 300 K and 1 bar to equilibrate the temperature and pressure, and to allow the dendrimer structures to relax. After this simulation, the dendrimer–water systems were subjected to two cycles of annealing. The annealing process was performed in the isothermal–isochoric ensemble (NVT). One annealing cycle proceeded as follows: A temperature ramp from 300 K to 500 K over 1 ns, holding the temperature at 500 K for 5 ns, a temperature ramp from 500 K to 300 K over 2 ns, and holding the temperature at 300 K for 2 ns. The annealed systems were allowed to relax for 10 ns at 300 K and 1 bar in the NpT ensemble.

B. Production Simulations

The dendrimer structures obtained after the annealing procedure were used to start both dendrimer–water and dendrimer–water–NPH simulations. We refer to the dendrimer–water and dendrimer–water–NPH systems as GX^{Wat} and GX^{NPH}, respectively. X represents the dendrimer generation in this nomenclature. NPH molecules were added at a distance of at least 2.0 nm from the dendrimer molecule in the starting configuration for the GX^{NPH} systems. The number of NPH molecules in each system varied to maintain a similar NPH/water ratio across all GX^{NPH} systems. We performed three replicates of each GX^{NPH} system, where the initial placement of the NPH and water molecules differed for each replicate. The final GX^{NPH} systems contained 1 dendrimer, 10–17 NPH molecules, 23336–40591 water molecules, and 32–256 counterions. The GX^{Wat} systems contained the same number of water molecules and counterions as their respective counterpart GX^{NPH} systems. Following energy minimizations and 1 ns equilibration runs in the NpT ensemble, 50 ns production runs were performed in the NpT ensemble for each system. Including the equilibration, annealing, and production simulations, we performed over 1 μs of simulations on 70,000+ atom systems to generate the results presented in this paper.

C. Simulation Details

MD simulations were performed with GROMACS v4.5.5 and GROMACS v5.0.2.[34] We used the leap-frog integrator with a time step of 2 fs. The system configurations were saved every 1 ps. Two thermostats were used: one to control the temperature of the dendrimer, and one to control the temperature of the NPH and water molecules. This strategy is commonly practiced to prevent the problem of "hot solvent cold solute" that arises in systems where there is imperfect energy exchange between the different components in a simulation.[35–37] Equilibration runs were performed with a Berendsen thermostat[38] and Berendsen barostat,[39] with τ =0.5 ps and τ =1.0 ps, respectively. Production runs were performed with a Nosé-Hoover thermostat[40] and Parrinello-Rahman barostat,[41] with τ =0.5 ps and τ=1.0 ps, respectively. Center of mass motion was removed every 100 steps. The cutoff distance for Lennard-Jones and Coulombic interactions was 1 nm. Bonds containing a hydrogen atom were constrained with the P-LINCS algorithm.[42] The long range electrostatic interactions were calculated with the particle mesh Ewald method.[43] Visual Molecular Dynamics[44] was used to perform visualization and generate all images of the simulation systems.

III. RESULTS AND DISCUSSION

We studied the association of NPH with G3–G6 PAMAM dendrimers using all-atom MD simulations with the goal of understanding how small aromatic entities interact with dendrimer hosts. In our previous work with the same system,[32] we reported increasing NPH association with increasing dendrimer generation from G3–G6, consistent with experimental results. We observed NPH–NPH interactions that stabilized the association of NPH with the dendrimers. We consider a NPH molecule associated if there are at least four heavy atom contacts between the NPH molecule and the dendrimer. The number of NPH molecules associated with the dendrimers over the last 20 ns of our production simulations were approximately 5, 7, 9, and 15 NPH molecules out of 10, 10, 11, and 17 NPH molecules present for the G3, G4, G5, and G6 dendrimer systems, respectively.

A. Dendrimer Structure

We calculated the size, shape, and terminal amine density profiles of the dendrimers for the GX^{Wat} and GX^{NPH} systems. The radii of gyration (R_g) of the dendrimers in water are within experimental values from SAXS[45] and SANS[46] studies. No change in dendrimer R_g was observed during NPH association for any dendrimer generation. The aspect ratios and asphericity of the dendrimers were similar to previous simulations of PAMAM dendrimers in water.[47] With the exception of the G3 dendrimer, which became slightly more spherical after the association of NPH, the sphericities of the dendrimers were the same with and without associated NPH molecules.

Beyond the dendrimer R_g and shape, another structural property of dendrimers is the extent of backfolding of the dendrimer branches. We consider a dendrimer branch to be backfolded if the geometric distance of each subsequent branch generation from the dendrimer center does not increase monotonically. Therefore, backfolding can be characterized by the distribution of terminal groups within the dendrimer volume. Since the terminal groups are located at the very end of the dendrimer branches, their spatial location within the dendrimer provides a measure of how much the dendrimer branches are folded back towards the center of the dendrimer. Researchers have hypothesized that backfolding may be an important part of the host–guest behavior of some hydrophobic molecules with dendrimers.[48] The density of the amine terminal groups as a function of the distance from the dendrimer center of geometry (for the remainder of this paper referred to as "dendrimer center") reveals that, under the solvent conditions studied in this work, the amine terminal groups are distributed throughout the dendrimer, with the highest density of groups inside the dendrimer R_g. The terminal amine density profiles are consistent with both experimental results, which have shown dendrimer terminal groups to be distributed throughout the interior for several different types of dendrimers,[49–51] and previous simulations of PAMAM dendrimers at neutral pH.[26] As demonstrated later and shown in previous work[52], the dendrimer branches (particularly terminal amine groups) do not have to be hidden from the solvent environment just because they are backfolded.

On average, there are no changes in the density distribution of the amine terminal groups when NPH molecules are associated with the dendrimers. This result suggests that the average level of backfolding does not change when NPH is associated with the

dendrimers. Backfolding may be important to the association of NPH molecules with dendrimers, however NPH association does not induce a change in the level of dendrimer backfolding. With the exception of a slight increase in the sphericity of the G3 dendrimer, we observe no change in the dendrimer size, shape, or level of backfolding during the association of NPH molecules. We hypothesize that since the NPH molecules are accommodated in the dendrimer through local structural changes, as described later in the paper, no changes in the measures of overall dendrimer structure are observed.

B. Location of NPH association

One key factor in dendrimer–guest interactions is the location of the guest association sites within the dendrimer structure. Understanding this feature of the interactions can help researchers design application–specific dendrimers by tuning dendrimer properties to optimize dendrimer–guest interactions. The location of guest association can be considered from several perspectives, including the geometric distance from the dendrimer center, chemical distance from the dendrimer center (i.e. branch subgeneration), and the location on a dendrimer branch (i.e. does the guest preferentially associate with certain chemical features of a given dendrimer branch).

The density of the dendrimer, water, and NPH molecules during the association are calculated as a function of the distance from the dendrimer center to understand the interplay between the dendrimer, water, and guest molecules. The density profiles for all GX^{NPH} systems are reported in Figure 1. The features of the dendrimer densities, including the development of a constant density region for the G6 dendrimer are generally consistent with previous simulations of PAMAM dendrimers using different force fields.[26,53,54] The dendrimer density profiles, in conjunction with the size, shape, and terminal group distribution suggest that the OPLS/AA force field provides a representation of PAMAM dendrimers which is consistent with experiments, theory, and simulations.

The density profiles of water in the GX^{NPH} systems reveal that there is similar water penetration into the G3–G6 dendrimers. In all cases, a small amount of water is able to penetrate to within 0.2 nm of the dendrimer center. As seen from Figure 1(c), some water penetrates all the way to the center of the G5 dendrimer. Such water penetration to the G5 dendrimer center was observed in two of the three replicates. Visual inspection shows

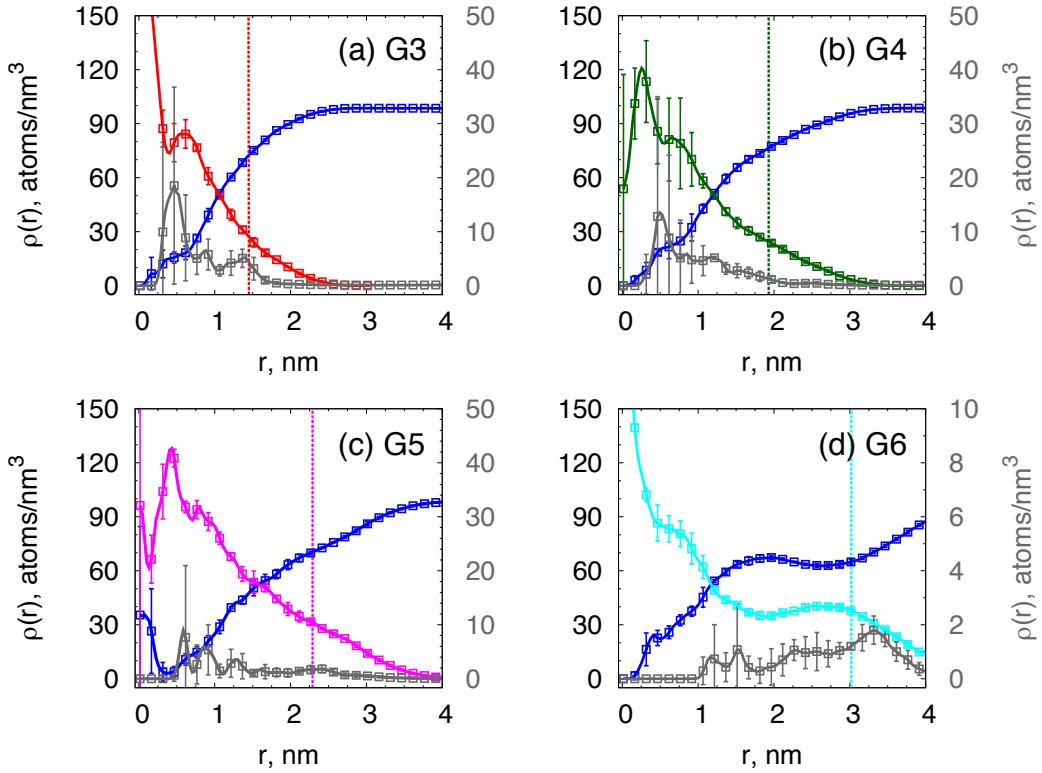

Figure 1. Radial density profiles of the dendrimer, NPH, and water as a function of distance from the dendrimer center of geometry. Dendrimer density (red, green, magenta, cyan), water density (blue), and NPH density (gray) for the (a) G3, (b) G4, (c) G5, and (d) G6 systems. Dendrimer and water density are read from the left axis, and NPH density is read from the right axis. Note the scale for the NPH density (right axis) for the G3, G4, and G5 dendrimers is different than the G6 dendrimer. All densities are averaged over the last 20 ns of the production simulations. Error bars represent the standard deviation of the averages between the three replicate production simulations. The dendrimer R_g's averaged over the last 20 ns of the production simulations are shown as the vertical dashed lines.

that water molecules become briefly trapped near the center of the G5 dendrimer. In both replicates of the $G5^{NPH}$ system with an increase in water density near the dendrimer center, fewer than 25 unique water molecules penetrated inside 0.2 nm from the dendrimer center over the last 20 ns of the simulations. We observe that the density of water within the G6 dendrimer (Figure 1(d)) from 1.5 to 3 nm (the constant density region of the G6 dendrimer) is about 2/3 of the bulk density of TIP3P water at 1 bar and 300 K (98.5 atoms/nm^3). Snapshots of the solvent accessible surface of the G6 dendrimer in Figure 2

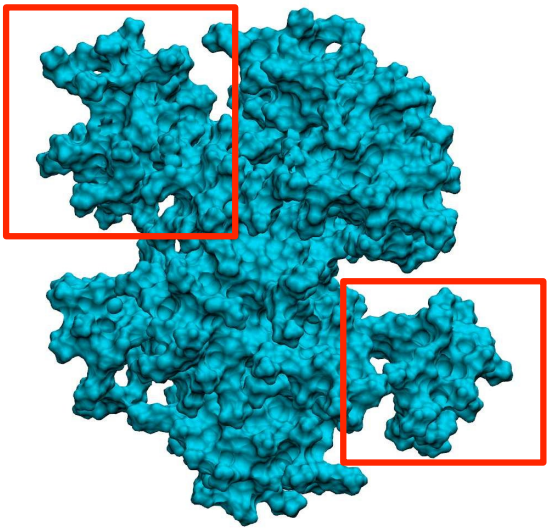

Figure 2. Snapshot of the G6 dendrimer (cyan) from a $G6^{NPH}$ simulation. The dendrimer is shown as the solvent accessible surface using a 0.14 nm probe. Example areas of locally high dendrimer density formed by clusters of dendrimer branches away from the dendrimer center are enclosed in red boxes.

lend insight into the structure of the dendrimer in the region from 1.5 to 3 nm from the dendrimer center. As shown by Figure 2 some of the dendrimer branches in this region appear to cluster together. The clusters extend towards the periphery of the dendrimer, with space between the different clusters. The result is that some areas between 1.5 and 3 nm of the dendrimer center have locally high dendrimer density and others have nearly zero dendrimer density. Water easily penetrates the areas with low dendrimer density, surrounding, but not penetrating into the clusters of dendrimer branches. The region from 1.5 to 3 nm from the G6 dendrimer center is therefore easily accessible to dissolved molecules (such as NPH), and contains potential association sites within the clusters of dendrimer branches. In this manner, dendrimer branches can be backfolded without being hidden from the solvent environment.

NPH penetration into the dendrimer structure decreases with increasing dendrimer generation. The maximum NPH density is within 0.5 nm of the dendrimer center for the G3 dendrimer, but outside of 1.0 nm from the dendrimer center for the G6 dendrimer. It should be noted that although the maximum *density* of NPH molecules is within 1 nm of the dendrimer center for the G3–G5 dendrimers, the maximum *number* of NPH molecules

associated with the G3–G5 dendrimers is centered near their R_g. The open structure of the G3 dendrimer allows some NPH molecules to diffuse to locations near the dendrimer center. In all three of the replicate simulations of the $G3^{NPH}$ system we observed NPH molecules associate within 0.5 nm of the dendrimer center. The $G4^{NPH}$ system only had one replicate with NPH associating inside of 0.5 nm from the dendrimer center, and none of the replicate simulations for the $G5^{NPH}$ and $G6^{NPH}$ systems showed association within 0.5 nm of their respective dendrimer centers. The water density profile for the G5 and G6 dendrimers indicate that NPH could likely find a path to diffuse to the center of the dendrimers. However, we hypothesize that the clusters of dendrimer branches shown in Figure 2 provide the NPH molecules adequate opportunities for association in the mid- and outer-regions of the dendrimer, and decrease the chances of NPH diffusing all the way to the dendrimer center. The transition in the NPH association behavior occurs around the G4 and G5 dendrimers. For those dendrimer generations, some NPH molecules are able to diffuse near the center of the dendrimers (< 0.5 nm), but increasing numbers of NPH molecules instead associate in the mid-regions of the dendrimer. Experimentally, the increase in the hydrophobicity of pyrene association sites in carboxylated PAMAM dendrimers occurred around G4,[16] the same generation that we observe a transition in the location of NPH association with PAMAM dendrimers. The onset of surface crowding, the creation of a constant density region, and the outward shift of NPH association sites may all be related.

As described above, we found that NPH molecules generally associate closer to the dendrimer center for lower generation dendrimers, and the association sites move towards the dendrimer mid- and outer- regions with increasing dendrimer generation. Since the dendrimer branches are backfolded, association closer to, or further from the dendrimer center does not provide an indication of which dendrimer subgenerations are most involved in the association of NPH molecules. To quantify the contribution of each subgeneration, we calculated the average number of heavy atom contacts between each dendrimer sub-generation and associated NPH molecules. The results are reported in Figure 3. In all cases we observe that the two outermost dendrimer subgenerations contribute over 65% of the total contacts. While this could be expected for dendrimers without any backfolding, in the case of PAMAM dendrimers where we observe significant backfolding, the largest contributions to NPH association from the outermost branches is intriguing.

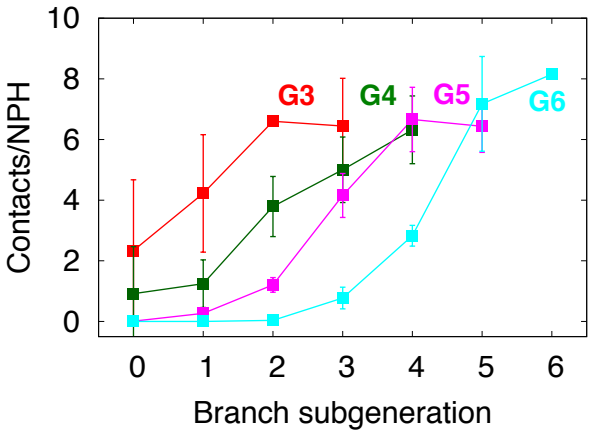

Figure 3. Number of heavy atom contacts between each dendrimer subgeneration and associated NPH molecules. The G3, G4, G5, and G6 dendrimer are shown as red, green, magenta, and cyan, respectively. The lines are to guide the eye. Error bars represent the standard deviation on the average of the three replicate simulations for each GX^{NPH} system.

It has been shown that the terminal groups of dendrimers have more mobility,[51] even when backfolded within the dendrimer structure. We hypothesize that the increased mobility of the outer subgenerations allows these portions of the dendrimer to cooperatively rearrange to accommodate NPH molecules. This suggests that backfolding plays an important role in the association process. Outer subgenerations have greater mobility, and the clusters of dendrimer branches in the mid-regions offer protection from a water environment. Backfolding therefore enables dendrimer branch mobility within the context of a protected environment. This likely contributes to the association of hydrophobic entities with dendrimers. Another observation is that the total number of contacts between the NPH and each dendrimer subgeneration is similar for all dendrimer generations, starting from the outermost subgeneration and moving towards the innermost. For example, the outermost subgeneration for each of the G3–G6 dendrimers has an average of about 6–8 contacts with each associated NPH molecule, and the second outermost subgeneration has an average of about 5–7 contacts with each associated NPH molecule. This result suggests similarities between the mechanism of association for dendrimers of varying size.

For many dendrimer host–guest interactions, researchers have observed local chemical preferences for guest association, such as dendrimer functionalities that interact with the guest through hydrogen bonding or ionic interactions. Since our study examines the association of a non-polar hydrophobic molecule there are no obvious favorable association

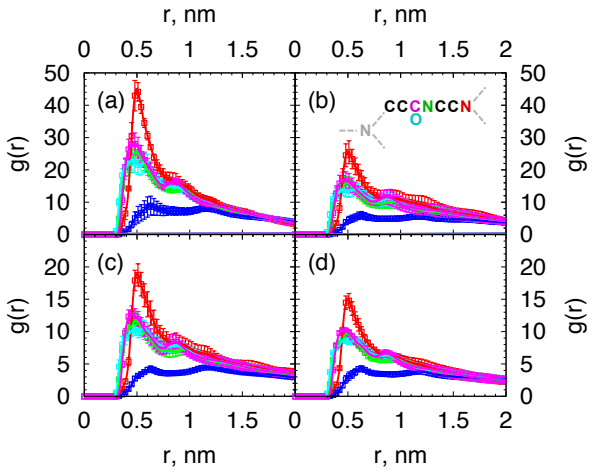

Figure 4. RDFs between different dendrimer atom types and NPH for the (a) G3, (b) G4, (c) G5, and (d) G6 PAMAM dendrimers. Colored atoms in the inset of panel (b) correspond with colors of the RDFs reported in panels (a)–(d). Tertiary amine–NPH (red), secondary amine–NPH (green), primary amine–NPH (blue), amide carbon–NPH (magenta), and amide oxygen–NPH (cyan) RDFs shown. All RDFs are calculated between the specified dendrimer atom type and the heavy atoms of the NPH molecules over the last 20 ns of the production simulations. Error bars represent the standard deviation of the average of the RDFs from the three replicate simulations.

sites. To test if there was a specific functional group or location which acted as a preferential association site for NPH, we selected several atoms along the dendrimer monomer repeat unit and calculated the atom–atom radial distribution function (RDF) between the selected dendrimer atom type and all of the heavy atoms of the NPH molecules. The different atoms along the dendrimer monomer unit from which we calculated the RDF are shown in the inset of Figure 4(b). The RDFs for the G3–G6 dendrimers are shown in Figure 4. Several features are immediately clear. The largest peak in any RDF is from the RDF between the tertiary amines of the dendrimer (where the dendrimer branches) and NPH, and the smallest peak of any RDF is between the primary amines (terminal groups) and NPH. The RDFs between the other atom types and NPH have intermediate peak heights. These results show that the NPH molecules preferentially associate near the tertiary amines. As noted earlier and shown with the diagram of PAMAM located in the inset of Figure 4(b), the tertiary amine is the location at which the dendrimer branches split and a new dendrimer generation begins. These sites are likely favorable

for NPH and other hydrophobic molecules because three dendrimer branches (two from generation $i+1$, and one from generation i) are always near each other. The proximity of the dendrimer branches allows them to cooperatively create an association site for NPH molecules which is protected from water.

The location near the tertiary amines and between branches of the dendrimer is the same association site as previously proposed from experiments with other guest molecules including phenanthrene,[55] 2-naphthol,[56] and phenylbutazone.[57] Phenanthrene is a polycyclic aromatic hydrocarbon like NPH, but with one additional fused aromatic ring. It is expected that the hydrophobic and similarly–sized phenanthrene may have the same association site as NPH. In contrast, 2-naphthol includes an alcohol group, resulting in reduced hydrophobicity compared with NPH. Kleinman et al. proposed that the alcohol from 2-naphthol interacts with the tertiary amine of PAMAM dendrimers.[56] Based on the results presented here, the location near the tertiary amine may also be favorable for the aromatic portions of 2-naphthol. From analysis of the NOE cross peaks from 2D-NOSEY NMR studies, Yang et al. showed that one encapsulation site for phenylbutazone was between dendrimer branches near the tertiary amines. Compared with the previous guest molecules, phenylbutazone is larger and more complex. It is an anti-inflammatory drug with two separated aromatic rings, an alkane chain, and a molecular weight greater than twice that of NPH and 2-naphthol. In light of these results, the location around the tertiary amine of PAMAM dendrimers appears to be a favorable association site for hydrophobic aromatic groups in general. Our results also show that although the two outermost dendrimer subgenerations have the most contacts with associated NPH molecules, the terminal groups themselves are the functionality least involved in the association of NPH with PAMAM dendrimers.

C. Local environment of the association site

We have shown that NPH molecules associate further from the dendrimer center with increasing dendrimer generation, that most contacts between associated NPH and dendrimers are with the two outermost dendrimer subgenerations, and that NPH molecules are more likely to associate at the dendrimer branch points. PAMAM dendrimers contain functional groups, including amine and carbonyl groups, that are not generally considered

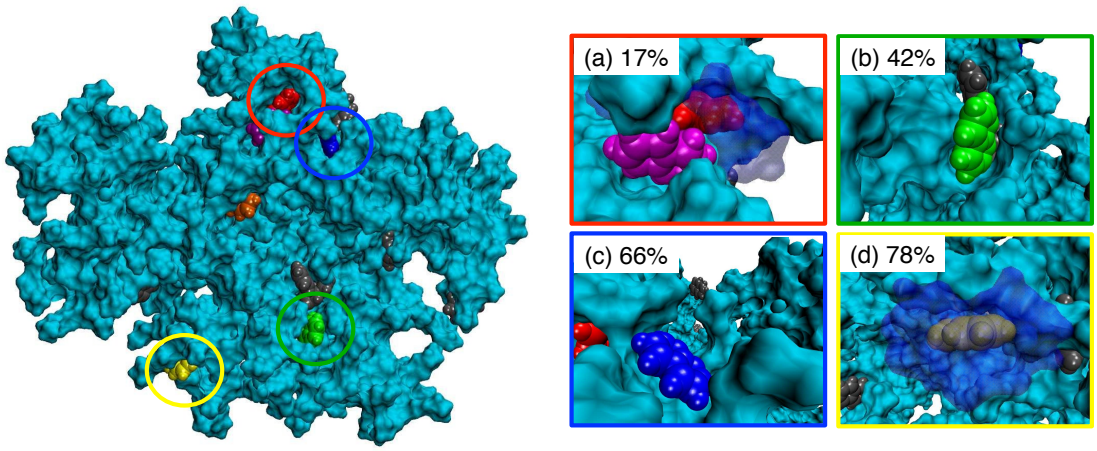

Figure 5. Examples of NPH association to a G6 dendrimer with a percent hydration of (a) 17%, (b) 42%, (c) 66%, and (d) 78%. The NPH molecule of interest is colored to match each box respectively. In panels (a) and (d), the water molecules in the first hydration shell are shown as a transparent surface around the NPH molecule of interest.

hydrophobic. Given this chemistry and water penetration well into the dendrimer interior (Figure 1), how does NPH, a small hydrophobic molecule, associate with PAMAM dendrimers? Visual inspection of the trajectories reveals that NPH molecules often associate within protected regions of the dendrimer structure that look like "pockets". We show several snapshots of NPH association in Figure 5. The NPH molecules in Figure 5(a)-(c) are in protected pocket-like structures. The pockets appear to be formed between or under dendrimer branches. However, there are no pre-formed pockets; though Figure 5 certainly shows NPH molecules in something akin to a pocket, the pockets do not exist before the NPH and dendrimer interact. NPH association with PAMAM dendrimers is dynamic due to the mobility of the dendrimer branches. There appears to be a cooperative interaction between the NPH molecules and dendrimer branches involving both NPH diffusion across the dendrimer structure and rearrangement of the dendrimer branches. Figure 6 shows the progression of the association of a NPH molecule over 10 ns. The location of the NPH molecule within the dendrimer and the local dendrimer structure around the NPH molecule evolve over time. In order to quantify the concept of a pocket and the local environment around associated NPH molecules, we calculated the percent hydration of associated NPH molecules. The percent hydration of each associated NPH molecule was determined by calculating the number of water molecules within its first hydration shell

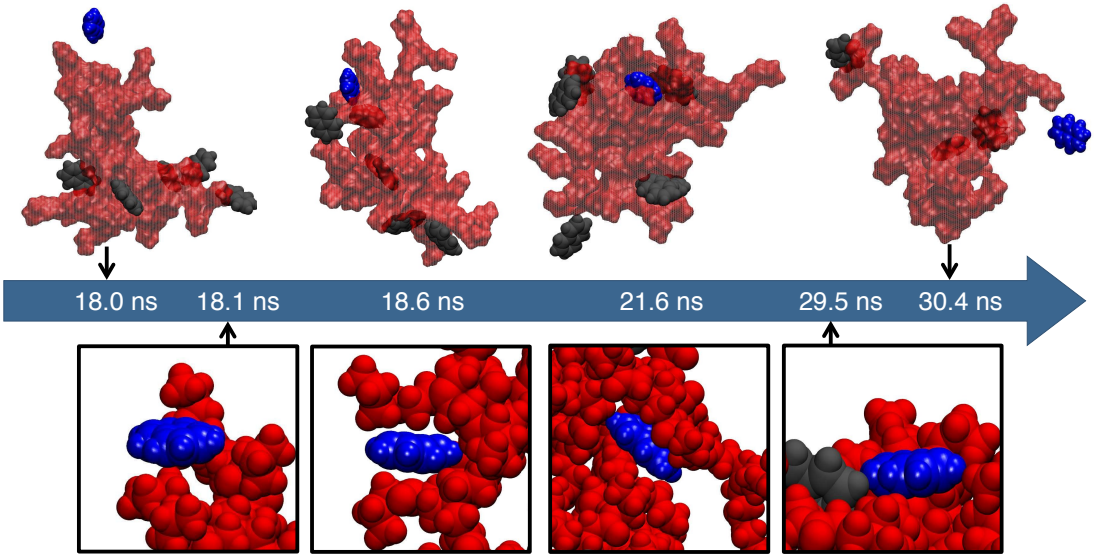

Figure 6. Example trajectory of the association of a NPH molecule with a G3 dendrimer. The bottom panels provide the zoomed in view of the top panels, focusing on the region around the NPH molecule of interest (blue).

and dividing it by the average number of water molecules in the first hydration shell of NPH in bulk water. The average number of water molecules within the first hydration shell of NPH in bulk water was calculated by numerically integrating the NPH–water RDF:

$$N_{wat} = 4\pi\rho_{wat}\int_{r=0}^{R} r^2 g(r)dr \quad (1)$$

where N_{wat} is the number of water molecules in the first hydration shell of NPH, ρ_{wat} is the bulk water density, R is the distance to the first minimum in the NPH–water RDF (0.704 nm), and $g(r)$ is the NPH–water RDF calculated from simulations of NPH in water only (no dendrimers). We found that many associated NPH molecules had a reduced number of water molecules in their first hydration shell, suggesting protected association sites. In Figure 5 we show representative examples of NPH association with the dendrimer and the percent hydration of each. It appears that when NPH molecules are protected from water by the dendrimer (or other NPH molecules, see Figure 5(a)) on both faces, the number of water molecules in the first hydration shell of the associated NPH molecule decreases by at least 50%.

The average percent hydration of NPH molecules associated with G3–G6 dendrimers all

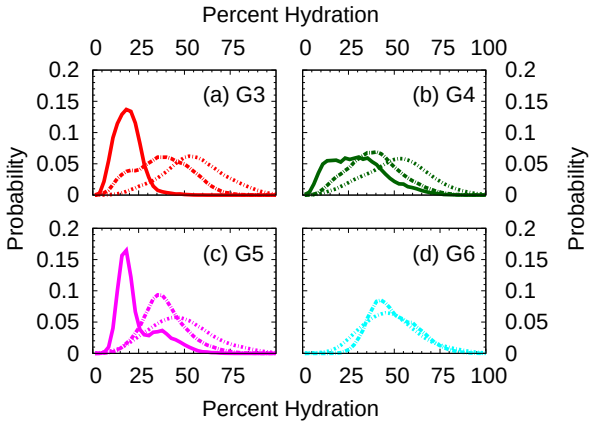

Figure 7. Distribution of the percent hydration of associated NPH molecules for the (a) G3, (b) G4, (c) G5, and (d) G6 dendrimers. Solid lines represent NPH associated in the inner region ($r < \frac{1}{3}R_g$), long-dashed lines represent NPH associated in the mid-regions ($\frac{1}{3}R_g < r < \frac{2}{3}R_g$), and the short-dashed lines represent NPH associated in the outer regions ($r > \frac{2}{3}R_g$). Inner region for G6 not shown due to inadequate sampling (< 50 observations with 1 NPH molecule).

fall between 40% and 50%. This suggests similarities in the local environment of NPH association sites for 3$^{\text{rd}}$–6$^{\text{th}}$ generation PAMAM dendrimers. Even though the G6 dendrimer (9412 atoms) is a much larger structure than the G3 dendrimer (1124 atoms), the NPH association appears to take place in similar protected pockets. Interestingly, the average percent hydration of associated NPH molecules indicates that NPH retains nearly 50% of its bulk hydration when associated with the dendrimers. If we consider the number of water molecules in the first hydration shell to be a measure of the hydrophobicity of the local environment around an associated NPH molecule, then on average, the association sites are relatively hydrophilic. Although this may be surprising for a hydrophobic molecule like NPH, experimental studies also found a relatively hydrophilic environment around pyrene molecules associated with PAMAM dendrimers.[16] The experimental studies also reported a slight increase in the hydrophobicity of the local environment of associated pyrene with increasing dendrimer generation. Our calculations of percent hydration do not capture any such trends. We note that the percent hydration may be an insufficient indicator of hydrophobicity to capture the small changes observed in experiments.

To ascertain if the percent hydration of a NPH molecule associated with the dendrimers is dependent on the associated molecule's distance from the dendrimer center, we divided

the dendrimer into three concentric regions. The inner region is defined as $r < \frac{1}{3}R_g$, the middle region is defined as $\frac{1}{3}R_g < r < \frac{2}{3}R_g$, and the outer region is defined as $r > \frac{2}{3}R_g$, where r is the distance from the dendrimer center. We calculated the distribution of the percent hydration for associated NPH molecules in each region. The results are reported in Figure 7. The width of the distribution indicates the range of percent hydration of associated NPH in each region. As seen in Figure 7, there is considerable overlap in the percent hydration for NPH molecules associated in the different regions. Below 50% hydration (examples in Figure 5(a)-(b)) does not require NPH to associate within the inner-, or even mid- regions of the dendrimer. The dendrimer branches are able to form pockets which offer a protected local environment for NPH association in the inner-, mid- and outer- regions.

NPH molecules associated in the inner regions of the G3–G5 dendrimers have lower percent hydration than NPH molecules associated in the mid- or outer-regions. However, NPH molecules associated within the inner region represent less than 4% of the total NPH association with the dendrimers. Most of the NPH molecules associated in the mid-regions of the dendrimers have a percent hydration between 10% and 75%. Some NPH molecules associated with the outer regions of the G3 and G4 dendrimers have nearly 100% of the water in their hydration shell, indicating the NPH molecules in this region are not associating in a pocket-like structure. Figure 5(d) provides an example of NPH association without a pocket-like structure. How can this type of association play a role in NPH–dendrimer interactions? The progression of a NPH molecule associating with the G3 dendrimer in Figure 6 provides one example. The molecule of interest (blue) approaches the dendrimer (t = 18.0 ns) and initially associates with the surface created by dendrimer branches (t = 18.1 ns). The molecule diffuses along the dendrimer surface (with a high percent hydration), interacting with the dendrimer branches. The branches rearrange allowing the molecule to move into a pocket-like structure (with a lower percent hydration) between dendrimer branches (t = 18.6 ns). The NPH remains associated in a pocket structure which continues to change with the motions of the dendrimer branches and NPH molecule (t = 18.6 ns – 29.5 ns) until the NPH molecule moves out of a region in between dendrimer branches (t = 29.5 ns). Once the NPH molecule is no longer in a protected pocket (t = 29.5 ns) for a period of time the molecule diffuses away from the dendrimer (t = 30.4 ns). Other times, NPH molecules diffuse away from the surface

Table I. Average percent hydration for NPH molecules that remain associated with the dendrimer for different lengths of time.

	Percent Hydration			
Time associated (ps)	G3	G4	G5	G6
5–50	78	74	76	79
50–100	62	60	59	63
100–500	56	54	53	55
500–1000	49	46	45	48
1000–2000	49	42	42	45
2000–4000	42	37	37	42
> 4000	33	33	35	35

of the dendrimer before the protected pocket is formed. Association with the surface of the outer branches appears to be responsible for the high percent hydration of associated NPH in the outer regions of the G3 and G4 dendrimers.

The G5 and G6 dendrimers have fewer associated NPH molecules with over 75% hydration in the outer regions of the dendrimer. As discussed earlier, the clustering of dendrimer branches into dense groupings in the outer dendrimer regions (see Figure 2) increases with increasing dendrimer generation. Association with high hydration in the outer regions is slightly reduced for the G5 and G6 dendrimers because it is more likely for a NPH molecule to associate at a location with locally high dendrimer density and multiple dendrimer branches. These branches can quickly rearrange to form a protected association site. As shown by the increasing overlap of the distributions for the mid- and outer- regions, the association with mid- and outer-regions of the dendrimer becomes increasingly similar for the G5 and G6 dendrimers. This may be related to formation of a constant dendrimer density region for the G6 dendrimer observed in Figure 1 and other simulation studies.[26,53,54]

Lower percent hydration of an associated NPH molecule indicates that the NPH molecule is more protected from the bulk water environment. Because NPH is a hy-

drophobic molecule, the association sites where NPH has a lower percent hydration should be more stable. We calculated the average percent hydration of NPH molecules over each continuous association event. Note that a single NPH molecule could have multiple association events over the course of a simulation. For example, a NPH molecule could associate with the dendrimer for 500 ps, then dissociate for a period of time, before re-associating with the dendrimer for another 200 ps. Each time the NPH molecule associated with the dendrimer was considered a separate association event. The association events were divided into the intervals shown in Table I based on the continuous length of the NPH association. We report the average percent hydration for each time interval. For all of the dendrimer generations studied, NPH molecules had a lower average percent hydration during longer lasting association events. This result suggests that association sites which reduce the number of water molecules in the first hydration shell of NPH, thereby protecting the associated NPH molecule from the bulk water environment, are better association sites for NPH. Taking the results of Table I and Figure 7 together, we see that the levels of percent hydration that correlate with association over even 1 ns (<40%) exist in the mid- and outer- regions of the dendrimers. NPH molecules do not need to penetrate to the innermost regions of the dendrimer structure to find an association site that will provide sufficient protection from the water environment. We note that an association with a low percent hydration does not guarantee that the molecule will remain associated for a longer period of time. The association may not last long due to other reasons (stress on the dendrimer structure, dendrimer branch rearrangement, etc). However, as shown by the values reported in Table I, NPH molecules associated with a high level of hydration are not likely to remain associated for more than a few hundred picoseconds. We also note that the average levels of percent hydration for the different length association events are strikingly similar across the different dendrimer generations. This suggests that the percent hydration of NPH is an important quantity in the association of NPH with dendrimers and shows the similarities in the mechanism of association of NPH with dendrimers of varying size.

To further investigate the role of backfolding on the percent hydration of associated NPH molecules, we performed simulations of the G3 and G4 dendrimers held fixed in an extended conformation. The simulations were performed under the same conditions (T,P, number of NPH molecules, water molecules, and counterions) and for the same length of

time as described in Section II. The average number of NPH molecules associated with the extended dendrimer was 1–3 molecules less than for the backfolded dendrimers, and the dendrimer branch point remained the most favored NPH association site. However, NPH molecules associated with the extended dendrimers showed a higher average percent hydration. Few association events lasted over 500 ps, and no association events lasted over 1 ns. In comparison, the backfolded G3 and G4 dendrimers had 60–100 association events over 500 ps and 20–50 association events over 1 ns. The lack of dendrimer backfolding prevented the dendrimer from forming protected pockets, which allow for longer-lasting association events. Though this preliminary work suggests the importance of backfolding for the association of hydrophobic molecules with dendrimers, future studies are warranted to decouple the effects of backfolding and dendrimer branch flexibility.

IV. CONCLUSIONS

A comprehensive description of the association of polyaromatic molecules with PAMAM dendrimers is developed using extensive MD simulations of NPH–PAMAM dendrimer–water systems. Our simulations revealed that the NPH–dendrimer association involved the cooperative formation of pocket-like structures by the dendrimer branches which enveloped NPH molecules and offered protection from the water environment. We quantified the concept of this pocket-like structure by calculating the percent hydration of associated NPH molecules as the number of water molecules in the first hydration shell of an associated NPH molecule divided by the average number of water molecules in the first hydration shell of a NPH molecule in bulk water. On average, NPH molecules that remained associated with the dendrimers for longer times had a lower percent hydration during the association event. Interestingly, NPH molecules can achieve a low percent hydration without penetrating well into the dendrimer. Similarities between the association of NPH, other aromatic molecules, and larger molecules containing aromatic groups with PAMAM dendrimers demonstrates the relevance of our results to applications involving more complex guest molecules. The insights from our work can be used to help design dendrimers for a variety of host–guest applications involving guests with hydrophobic and aromatic moieties.

V. ACKNOWLEDGMENTS

S.S. gratefully acknowledges financial support from Clemson University start-up funds. R.S.D. acknowledges support from NSF-funded CI-SEEDS grant #1212680, the Clemson University College of Engineering and Science, and the Clemson University Calhoun Honors College. We would like to acknowledge Drs. Pu Chun Ke, Priyanka Bhattacharya, and Nicholas K. Geitner for their comments on a draft of this manuscript. We thank the Clemson Cyberinfrastructure Technology Integration group for allocation of computing time on the Palmetto Cluster.

Graphical Abstract

Dendrimer pockets enable association by reducing naphthalene hydration even near the dendrimer periphery.

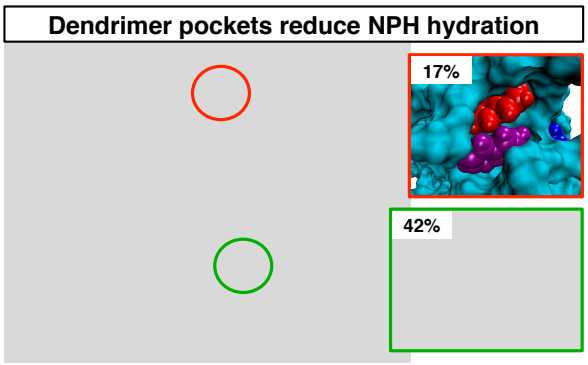

[1] D. A. Tomalia, *Prog. Polym. Sci.*, 2005, **30**, 294 – 324.

[2] P. Kesharwani, K. Jain and N. K. Jain, *Prog. Polym. Sci.*, 2014, **39**, 268 – 307.

[3] A. R. Menjoge, R. M. Kannan and D. A. Tomalia, *Drug Discov. Today*, 2010, **15**, 171 – 185.

[4] R. Esfand and D. A. Tomalia, *Drug Discov. Today*, 2001, **6**, 427–436.

[5] M. Arkas, D. Tsiourvas and C. M. Paleos, *Chem. Mater.*, 2003, **15**, 2844–2847.

[6] P. Bhattacharya, N. K. Geitner, S. Sarupria and P. C. Ke, *Phys. Chem. Chem. Phys.*, 2013, **15**, 4477–4490.

[7] V. Balzani, S. Campagna, G. Denti, A. Juris, S. Serroni and M. Venturi, *Accounts Chem. Res.*, 1998, **31**, 26–34.

[8] A. Adronov, S. L. Gilat, J. M. J. Frchet, K. Ohta, F. V. R. Neuwahl and G. R. Fleming, *J. Am. Chem. Soc.*, 2000, **122**, 1175–1185.

[9] M. M. Hann, A. R. Leach and G. Harper, *J. Chem. Inf. Comp. Sci.*, 2001, **41**, 856–864.

[10] J. Hu, T. Xu and Y. Cheng, *Chem. Rev.*, 2012, **112**, 3856–3891.

[11] I. Tanis and K. Karatasos, *J. Phys. Chem. B*, 2009, **113**, 10984–10993.

[12] Y. Cheng, Y. Li, Q. Wu, J. Zhang and T. Xu, *Eur. J. Med. Chem.*, 2009, **44**, 2219 – 2223.

[13] M. Lard, S. H. Kim, S. Lin, P. Bhattacharya, P. C. Ke and M. H. Lamm, *Phys. Chem. Chem. Phys.*, 2010, **12**, 9285–9291.

[14] M. Ballauff and C. N. Likos, *Angew. Chem. Int. Edit.*, 2004, **43**, 2998–3020.

[15] M. Baars and E. Meijer, *Dendrimers II*, Springer Berlin Heidelberg, 2000, vol. 210, pp. 131–182.

[16] G. Caminati, N. J. Turro and D. A. Tomalia, *J. Am. Chem. Soc.*, 1990, **112**, 8515–8522.

[17] J. Lim, G. M. Pavan, O. Annunziata and E. E. Simanek, *J. Am. Chem. Soc.*, 2012, **134**, 1942–1945.

[18] A. M. Jolly and M. Bonizzoni, *Macromolecules*, 2014, **47**, 6281–6288.

[19] J. D. Epperson, L.-J. Ming, B. D. Woosley, G. R. Baker and G. R. Newkome, *Inorg. Chem.*, 1999, **38**, 4498–4502.

[20] U. Boas, S. H. M. Sntjens, K. J. Jensen, J. B. Christensen and E. W. Meijer, *ChemBioChem*, 2002, **3**, 433–439.

[21] M. Pittelkow, J. B. Christensen and E. W. Meijer, *J. Polym. Sci. A1*, 2004, **42**, 3792–3799.

[22] J. Hu, Y. Cheng, Q. Wu, L. Zhao and T. Xu, *J. Phys. Chem. B*, 2009, **113**, 10650–10659.

[23] W.-d. Tian and Y.-q. Ma, *Chem. Soc. Rev.*, 2013, **42**, 705–727.

[24] N. Martinho, H. Florindo, L. Silva, S. Brocchini, M. Zloh and T. Barata, *Molecules*, 2014, **19**, 20424–20467.

[25] P. K. Maiti, T. Cağin, G. Wang and W. A. Goddard III., *Macromolecules*, 2004, **37**, 6236–6254.

[26] P. K. Maiti, T. Cağin, S. Lin and W. A. Goddard III., *Macromolecules*, 2005, **38**, 979–991.

[27] S. Lin, P. K. Maiti and W. A. Goddard III, *J. Phys. Chem. B*, 2005, **109**, 8663–8672.

[28] Y. Liu, V. S. Bryantsev, M. S. Diallo and W. A. Goddard III, *J. Amer. Chem. Soc.*, 2009, **131**, 2798–2799.

[29] V. Jain, V. Maingi, P. K. Maiti and P. V. Bharatam, *Soft Matter*, 2013, **9**, 6482–6496.

[30] W. L. Jorgensen, D. S. Maxwell and J. Tirado-Rives, *J. Am. Chem. Soc.*, 1996, **118**, 11225–11236.

[31] W. L. Jorgensen, J. Chandrasekhar, J. D. Madura, R. W. Impey and M. L. Klein, *J. Chem. Phys.*, 1983, **79**, 926–935.

[32] R. S. DeFever, N. K. Geitner, P. Bhattacharya, F. Ding, P. C. Ke and S. Sarupria, *Environ. Sci. Technol.*, 2015, **49**, 4490–4497.

[33] R. C. van Duijvenbode, M. Borkovec and G. J. M. Koper, *Polymer*, 1998, **39**, 2657–2664.

[34] S. Pronk, S. Pall, R. Schulz, P. Larsson, P. Bjelkmar, M. R. Apostolov, J. C. Smith, P. M. Kasson, D. van der Spoel, B. Hess and E. Lindahl, *Bioinformatics*, 2013, **29**, 845–854.

[35] D. Young, *Computational Chemistry: A Practical Guide for Applying Techniques to Real World Problems*, Wiley, 2004.

[36] D. van der Spoel, E. Lindahl, B. Hess, A. R. van Buuren, E. Apol, P. J. Meulenhoff, D. P. Tieleman, A. L. T. M. Sijbers, K. A. Feenstra, R. van Drunen and H. J. C. Berendsen, *Gromacs User Manual version 4.5.6*, 2010.

[37] M. Lingenheil, R. Denschlag, R. Reichold and P. Tavan, *J. Chem. Theory Comput.*, 2008, **4**, 1293–1306.

[38] H. J. C. Berendsen, J. P. M. Postma, W. F. van Gunsteren, A. DiNola and J. R. Haak, *J. Chem. Phys.*, 1984, **81**, 3684–3690.

[39] H. J. C. Berendsen, J. P. M. Postma, W. F. van Gunsteren, A. DiNola and J. R. Haak, *J.*

Chem. Phys., 1984, **81**, 3684–3690.

[40] S. Nosé, *Mol. Phys.*, 1984, **52**, 255–268.

[41] M. Parrinello and A. Rahman, *J. Appl. Phys.*, 1981, **52**, 7182–7190.

[42] B. Hess, *J. Chem. Theory Comput.*, 2008, **4**, 116–122.

[43] U. Essmann, L. Perera, M. L. Berkowitz, T. Darden, H. Lee and L. G. Pedersen, *J. Chem. Phys.*, 1995, **103**, 8577–8593.

[44] W. Humphrey, A. Dalke and K. Schulten, *J. Mol. Graphics*, 1996, **14**, 33–38.

[45] S. Rathgeber, M. Monkenbusch, M. Kreitschmann, V. Urban and A. Brulet, *J. Chem. Phys.*, 2002, **117**, 4047–4062.

[46] L. Porcar, Y. Liu, R. Verduzco, K. Hong, P. D. Butler, L. J. Magid, G. S. Smith and W. Chen, *J. Phys. Chem. B*, 2008, **112**, 14772–14778.

[47] V. Maingi, V. Jain, P. V. Bharatam and P. K. Maiti, *J. Comput. Chem.*, 2012, **33**, 1997–2011.

[48] N. Shao, T. Dai, Y. Liu, L. Li and Y. Cheng, *Soft Matter*, 2014, **10**, 9153–9158.

[49] S. Rosenfeldt, N. Dingenouts, M. Ballauff, N. Werner, F. Vgtle and P. Lindner, *Macromolecules*, 2002, **35**, 8098–8105.

[50] K. L. Wooley, C. A. Klug, K. Tasaki and J. Schaefer, *J. Am. Chem. Soc.*, 1997, **119**, 53–58.

[51] C. B. Gorman, M. W. Hager, B. L. Parkhurst and J. C. Smith, *Macromolecules*, 1998, **31**, 815–822.

[52] L. Yang and S. R. P. Da Rocha, *Mol. Pharm.*, 2014, **11**, 1459–1470.

[53] K. Karatasos, D. B. Adolf and G. R. Davies, *J. Chem. Phys.*, 2001, **115**, 5310–5318.

[54] P. K. Maiti, Y. Li, T. Cağin and W. A. Goddard, *J. Chem. Phys.*, 2009, **130**, 144902.

[55] P. Chen, Y. Yang, P. Bhattacharya, P. Wang and P. C. Ke, *J. Phys. Chem. C*, 2011, **115**, 12789–12796.

[56] M. H. Kleinman, J. H. Flory, D. A. Tomalia and N. J. Turro, *J. Phys. Chem. B*, 2000, **104**, 11472–11479.

[57] W. Yang, Y. Li, Y. Cheng, Q. Wu, L. Wen and T. Xu, *J. Pharm. Sci.*, 2009, **98**, 1075–1085.